JOURNAL OF THERMOPHYSICS AND HEAT TRANSFER
Vol. 7, No. 2, April–June 1993

Thermodynamic Properties of Molecular Hydrogen Plasma in Thermal and Chemical Nonequilibrium

Kuan Chen*
University of Utah, Salt Lake City, Utah 84112
and
Thomas L. Eddy†
EG & G Idaho, Idaho Falls, Idaho 83415

A nonequilibrium plasma model is developed for computing the thermodynamic properties of partially ionized molecular hydrogen in both non-local thermal equilibrium (non-LThE) and non-local chemical equilibrium (non-LChE). The model uses multitemperatures for thermal nonequilibrium. Nonzero chemical affinities are used as a measure of the deviation from chemical equilibrium. Internal energy, enthalpy, entropy, Gibbs and Helmholtz free energies, and the speed of sound are computed for pressures ranging from 0.1 to 100 kPa, and electron translational temperatures ranging from 5000 to 35,000 K. Effects of the changes in pressure, chemical affinity, and temperatures of different energy modes and species on the thermodynamic properties of molecular hydrogen are examined and discussed. It is found that a positive affinity of the recombination reaction or a decrease in plasma pressure will cause ionization to occur at lower temperatures, resulting in higher plasma enthalpy, internal energy, and entropy. Increase of the temperature of a particular energy mode also increases the total energy and entropy of the plasma, but the translational temperatures play a dominant role in the temperature range considered. The speed of sound is changed more by chemical nonequilibrium than by thermal nonequilibrium effects.

Nomenclature

A, a = Helmholtz free energy
C = concentration
c = speed of sound
c_p = constant-pressure specific heat
e = electronic charge
e^- = free electron
G, g = Gibbs free energy
H, h = enthalpy
H_r^0 = negative of the heat of reaction for reaction r
$\hbar$ = Planck's constant
I = moment of inertia
k = Boltzmann's constant
m = mass
N = total particle number
n = number density
p = pressure
q = heat
R = gas constant
S, s = entropy
T = temperature
U, u = internal energy
V = volume
v = specific volume
w = work
Z = partition function
z = number of elementary charges
α_r = chemical affinity for reaction r
γ = specific heat ratio
Δh = enthalpy of formation
θ = characteristic temperature
κ_f = forward rate constant
μ = chemical potential
ν = stoichiometric coefficient
ξ = extent of chemical reaction
ρ_D = Debye length
σ = intermolecular potential constant
ω = forward reaction rate

Subscripts
a = heavy particles
corr = Debye - Huckel correction
e = electron
int = internal energy modes
j = species j
r = rotational energy mode
t = translational energy mode
v = vibrational energy mode
x = electronic excitation energy mode

Introduction

MODELING of nonequilibrium plasma for advanced propulsion research has received increasing attention in recent years. In high-temperature propulsion systems such as gas-core and nuclear-thermal thrusters, the high gas velocity and low gas density in the thruster nozzle result in both local thermal and chemical nonequilibrium. Plasma property calculations based on local thermodynamic equilibrium (LTE) or frozen flow assumptions may result in significant errors for gas dynamics and heat transfer analyses in the design of advanced propulsion systems. It was mentioned in Pierce's book[1] that in the case of a hypersonic nozzle flow, the gas state is continuously changing and chemical nonequilibrium exists over large flow distances. As a result, three regions of flow are commonly assumed in the analysis of hypersonic nozzle flow: 1) an equilibrium flow in the converging portion and the throat of the nozzle due to the relatively low flow velocities; 2) a frozen flow region far downstream of the diverging section in which the composition is invariant; and 3) a region down-

Presented as Paper 91-1489 at the AIAA 22nd Fluid Dynamics, Plasma Dynamics, and Laser Conference, Honolulu, HI, June 24–26, 1991; received Dec. 27, 1991, revision received April 29, 1992; accepted for publiction June 3, 1992.

*Associate Professor, Mechanical Engineering Department. Member AIAA.
†Principal Engineer, Idaho National Engineering Laboratory. Member AIAA.

stream of the throat where chemical nonequilibrium exists. Flows in these regions have quite different characteristics and should be treated separately.

Most gas dynamics codes currently available for rocket engine design have taken chemical nonequilibrium into account by solving the stiff chemical rate equations directly. Early methods for chemical nonequilibrium used steady-state kinetics analysis which encountered a saddle-point singularity near the nozzle throat, making it difficult to integrate from the subsonic to the supersonic regions.[2] The time-dependent, finite-difference method by Anderson[2] alleviates the difficulty encountered with steady-state kinetics analysis. However, uncertainty in the rate constants and the stiff reaction rate equations make it difficult and sometimes inaccurate to compute chemically reacting flows at high temperatures. On the other hand, nearly constant chemical affinity was observed in several plasma jet and plume measurements,[3] indicating that it may be simpler and more accurate to use chemical affinity in thermodynamic analysis of high-temperature gas flow,[3] or to correct reaction rate equations for nonequilibrium.[4]

Thermal nonequilibrium implies that the temperatures of different species and energy modes (translational, rotational, vibrational, and electronic excitation) in a gas mixture are not equal. Vibrational nonequilibrium is of particular interest in the analysis of modern gasdynamic and chemical lasers, and has been an important aspect of hypersonic wind tunnels.[2] The two-temperature plasma model (which assumes the translational temperatures of electrons and heavy particles are different) is commonly used for the study of nonequilibrium plasma flow. Complete thermal nonequilibrium has not been considered in most gas dynamics analyses. Since at high temperatures, thermal nonequilibrium may have significant effects on emission coefficients and radiation emission is important to high-temperature gas measurement and diagnosis, gas dynamics analysis should include thermal nonequilibrium when applied to propulsion systems operating at very high temperatures and velocities.

Presented in this article is a nonequilibrium plasma model for computing the thermodynamic properties of partially ionized molecular hydrogen in both non-local thermal equilibrium (non-LThE) and non-local chemical equilibrium (non-LChE). Hydrogen is selected in the present investigation because it is the favored propellant fuel in advanced nuclear-thermal propulsion. Composition, partition functions, and thermodynamic properties of hydrogen have been investigated and calculated by several researchers. Most of the early works[5–10] were limited to LTE hydrogen. Sonic speed and chemical composition of low-temperature hydrogen were calculated by King[11] for LTE and frozen flows. Thermodynamic and transport properties for hydrogen in LChE were computed in Cho's thesis[12] with translational and electronic excitation nonequilibria taken into account. The LTE result of Cho's calculation agrees well with Patch's calculation[13] for temperatures above 2000 K.

In the present investigation, the nonequilibrium plasma model developed by Cho and Eddy[12] is modified to include chemical nonequilibrium. In addition, rotational and vibrational nonequilibria of diatomic and polyatomic components are added to the non-LThE model. The computed hydrogen properties show that a positive affinity of the recombination reaction or a decrease in pressure will cause ionization to occur at lower temperatures, resulting in higher plasma energy and entropy. Thermal nonequilibrium strongly affects internal energy, enthalpy, and entropy when chemical reactions take place. Gibbs and Helmholtz free energies are less sensitive to chemical and thermal nonequilibrium, but are affected strongly by pressure change at high temperatures.

Nonequilibrium Plasma Model

A nonequilibrium plasma model based on the generalized multithermodynamic equilibrium (GMTE) model was developed by Cho and Eddy[12] for a hydrogen plasma with translational and electronic excitation nonequilibria. The model uses multitemperatures for thermal nonequilibrium. It has been modified and extended to non-LChE gases[14,15] by using non-zero chemical affinities as a measure of the deviation from chemical equilibrium after rediscovered work of de Donder[16] and Prigogine,[17] as well as Potapov.[18] In addition, separate internal partition functions are employed for diatomic and polyatomic species in the modified plasma model. Consequently the assumption of equivalence between any translational, rotational, vibrational, or electronic excitation temperatures for different species is not necessary in the application of the present plasma model.

In the present nonequilibrium plasma model, chemical composition and thermodynamic properties of a hydrogen plasma at given pressure and chemical affinity are expressed as a function of different energy distribution parameters (temperatures) within each energy mode of each species. The heavy particles in the plasma are assumed to have the same translational temperatures. Therefore, the different temperatures involved are electron translational temperature T_e, translational temperature of the heavy particles T_a, rotational temperatures of diatomic and polyatomic species $T_{r,j}$, vibrational temperatures of diatomic and polyatomic species $T_{v,j}$, and electronic excitation temperatures $T_{x,j}$. The species considered in the present plasma model include hydrogen atom (H), proton (H^+), free electron (e^-), hydrogen molecule (H_2), negative hydrogen ion (H^-), hydrogen diatomic molecule ion (H_2^+), and hydrogen triatomic molecular ion (H_3^+).

The plasma is treated as an ideal gas with the Debye-Huckel approximation employed for pressure correction. The cutoff levels for the ionizations of H and H_2 are calculated by the Debye-Huckel method[19,20] and the modified Bethe method,[10,21] and the lower level of these two methods is used. The proration method after Patch[10] is used when the cutoff energy level is between two discrete levels.

The chemical affinity as defined by de Donder[16] is

$$\alpha = -\sum_j \mu_j \nu_j \tag{1}$$

The summation on the right side is one form of the law of mass action, which for chemical equilibrium is equal to zero; therefore, α is a measure of the deviation from the chemical equilibrium condition. The Gibbs free energy is related to the affinity by[4,22–24]

$$\mathrm{d}g|_{T,p} = \sum_j \mu_j \nu_j \,\mathrm{d}\xi = -\alpha \,\mathrm{d}\xi \tag{2}$$

Equation (2) shows that the affinity is the nonequilibrium driving potential operating through the nonequilibrium ξ attempting to bring the reaction into the equilibrium composition at the local temperature and pressure.[22] The $\mathrm{d}g = -\alpha \,\mathrm{d}\xi$ term is analogous to $\mathrm{d}w = -p \,\mathrm{d}v$ working or $\mathrm{d}q = T \,\mathrm{d}s$ heating. The sign of the affinity in relaxing recombinations is like that of the free energy for strongly reactive combinations, both having negative values. In the explicit statements of the law of mass action, the heat of reaction, dissociation, or ionization energy appears with the affinity, such that the difference represents the effective activation energy. As a result, it is convenient to use a dimensionless of reduced chemical affinity α^*, defined as

$$\alpha^* = \frac{\alpha}{H^0} = -\sum_j \frac{\mu_j \nu_j}{H^0} \tag{3}$$

where H^0 is the negative of the heat of reaction. In this work, the basis is the negative of the heat of reaction at 0 K and 100 kPa.

ξ is the extent of reaction with $\mathrm{d}\xi/\mathrm{d}t$, called the overall reaction rate or reaction velocity.[4,23] The rate of change of

species j is related to the overall reaction rate and chemical kinetics by

$$\frac{d\xi}{dt} = -\frac{1}{\nu_j}\frac{dN_j}{dt} = \omega\left\{1 - \exp\left[\frac{-\alpha}{kT}\right]\right\} \tag{4}$$

where the forward reaction rate is

$$\omega = \kappa_f \prod_{\text{reactants}} C_j^{\nu_j} \tag{5}$$

The chemical affinity is a parameter that can be used to quantify the degree of partially frozen flow. It can be directly entered into the thermodynamic diagnostic model equations[3,25] and evaluated, or it can be back-calculated from chemical kinetic measurements of the overall and forward reaction rates. The choice is a matter of convenience. The affinity provides a way for more precision to specify the reaction since the $\omega \exp[-\alpha/(kT)]$ term is the actual backward reaction rate, and not one based on backward rate coefficients calculated from the forward rate and the equilibrium constant.

Plots of thermodynamic data are provided so the reader can appreciate the effect of chemical nonequilibrium on the thermodynamic properties. The affinity is used similarly to equilibrium intensive variables. Actual processes would be expected to cross over "isaffins" (lines of constant affinity). Experimental work in argon[3] and argon/helium[25] plasma jets and hydrogen tunnel arc flows (unpublished results obtained by second author) have indicated that the affinity is essentially constant (frozen) at various radii, axial lengths, and at various power levels in the plasma plume, but has different values for different mixtures of gases. In this special case, the process would follow an isaffin on the chart. Just as a throttling process is isenthalpic, it appears that plasma free jets may be isaffinic. The thermodynamic plots as a function of the affinity are important in understanding the introduction and role of a new thermodynamic variable.

The chemical reactions considered are the formations of the five minor species from the collisions of the two major species of the seven components in hydrogen plasma. At high temperatures the two major species are H^+ and e^-. When the number density of H^+ drops below that of H, the major species are changed to H and e^-. In view of the large variety of the combinations of pressure, affinity, and different temperatures, we limited our attention to the cases in which α^* are the same for the five chemical reactions, $T_{x,j} = T_{x,H}$, and $T_{r,j} = T_{v,j} = T_a$. Although the plasma model we developed is capable of dealing with rotational and vibrational nonequilibria, the number densities of the diatomic and polyatomic species are very small for temperatures above 5000 K. Therefore, rotational and vibrational nonequilibria are expected to have little effects on plasma properties at high temperatures.

Hydrogen composition and partition functions have been calculated by the authors and Cho in a recent DOE report[14] for pressures ranging from 0.1 to 100 kPa, T_e from 5000 to 35,000 K, T_e/T_a from 1.0 to 1.4, and $T_e/T_{x,H}$ from 0.8 to 1.4. Three α^* values, 0, 0.2, and 0.4, were used in these calculations. Part of these results were presented and discussed in Ref. 15. It was found that the number density ratios of the minor species vary almost exponentially with variations in α^*. The total number density and the number densities of the major species are less sensitive to the change of affinity value because they have the baseline dependence on pressure and temperature.

Calculation of Thermodynamic Properties

Number densities and partition functions calculated from the non-LTE, non-LChE plasma model are used to compute thermodynamic properties A, G, H, S, and U for molecular hydrogen plasma at different pressures and temperatures. For a plasma in non-LThE, the temperatures of different species and energy modes are different. The ensemble average is used for computing the properties of the whole system. The ensemble properties are calculated by summing the properties of each species and each energy mode over all modes and species. For example, the internal energy of the plasma is calculated from

$$U = \sum_j \sum_k U_{k,j} + U_{\text{corr}} \tag{6}$$

where subscripts j and k represent the number of species and the number of energy modes, respectively. U_{corr} is the correction due to the Debye-Huckel approximation. Other thermodynamic properties are calculated in a similar fashion. Capitalized letters are used for properties per unit mass, and lower-case letters for properties per particle. The reference energy state is atomic hydrogen at 0 K and 100 kPa.

It is assumed that each species in the gas mixture behaves as an ideal gas, with the Debye-Huckel correction included in the translational mode. The energy modes considered in thermodynamic property calculation are the translational, rotational, vibrational, and electronic excitation modes. Each mode is considered as a Maxwell-Boltzmann system and is characterized by a temperature $T_{k,j}$ in complete multithermal equilibrium (MThE). NonBoltzmann distributions can be handled with partial MThE considerations. The Debye-Huckel approximation is employed because of the interaction of the charged particles in plasmas. Contributions of different energy modes are computed from the following equations:

1) Translational mode

$$a_{t,j} = -kT_{t,j}[\ln(Z_{t,j}/N_j) + 1] + a_{\text{corr},j} \tag{7}$$

$$g_{t,j} = a_{t,j} + p_j v_j \tag{8}$$

$$s_{t,j} = -\left.\frac{\partial a_{t,j}}{\partial t_{t,j}}\right|_{v_j} = k\left[\ln\left(\frac{Z_{t,j}}{N_j}\right) + 2.5\right] - \left.\frac{\partial a_{\text{corr},j}}{\partial T_{t,j}}\right|_{v_j} \tag{9}$$

$$u_{t,j} = a_{t,j} + T_{t,j}s_{t,j} \tag{10}$$

$$h_{t,j} = u_{t,j} + p_j v_j \tag{11}$$

2) Internal modes

$$a_{\text{int},j} = -kT_{\text{int},j}\ln Z_{\text{int},j} \tag{12}$$

$$g_{\text{int},j} = a_{\text{int},j} \tag{13}$$

$$s_{\text{int},j} = \left.\frac{-\partial a_{\text{int},j}}{\partial T_{\text{int},j}}\right|_{v_j} = k\ln Z_{\text{int},j} + kT_{\text{int},j}\left.\frac{\partial \ln Z_{\text{int},j}}{\partial T_{\text{int},j}}\right|_{v_j} \tag{14}$$

$$u_{\text{int},j} = a_{\text{int},j} + T_{\text{int},j}s_{\text{int},j} = kT_{\text{int},j}^2\left.\frac{\partial \ln Z_{\text{int},j}}{\partial T_{\text{int},j}}\right|_{v_j} \tag{15}$$

$$h_{\text{int},j} = u_{\text{int},j} \tag{16}$$

The translational partition function in the above equations is

$$Z_{t,j} = V(2\pi m_j kT_{t,j}/h^2)^{3/2} \tag{17}$$

Thus

$$Z_{t,j}/N_j = v_j(2\pi m_j kT_{t,j}/h^2)^{3/2} \tag{18}$$

where v_j is the specific volume of species j.

Only diatomic and polyatomic species have rotational and vibrational modes. If the coupling effects of these two modes are neglected, the rotational partition functions and their de-

rivatives can be calculated from

for $j = H_2$ or H_2^+

$$Z_{r,j} = T_{r,j}/(\sigma_j \theta_{r,j}) \tag{19}$$

$$\frac{\partial \ln Z_{r,j}}{\partial T_{r,j}} = \left(\frac{\partial Z_{r,j}}{\partial T_{r,j}}\right)\left(\frac{1}{Z_{r,j}}\right) = \frac{1}{T_{r,j}} \tag{20}$$

for $j = H_3^+$

$$Z_{r,j} = 8\pi^2(2\pi k)^{3/2}(I_A I_B I_C)^{1/2}/(\sigma_j \hbar^3) \times T_{r,j}^{3/2} \tag{21}$$

$$\frac{\partial \ln Z_{r,j}}{\partial T_{r,j}} = \frac{1.5}{T_{r,j}} \tag{22}$$

The vibrational partition functions and their derivatives are

for $j = H_2$ and H_2^+

$$Z_{v,j} = 1/[1 - \exp(-\theta_{v,j}/T_{v,j})] \tag{23}$$

$$\frac{\partial \ln Z_{v,j}}{\partial T_{v,j}} = \left(\frac{\theta_{v,j}}{T_{v,j}^2}\right)\exp\left(\frac{-\theta_{v,j}}{T_{v,j}}\right)\Big/\left[1 - \exp\left(\frac{-\theta_{v,j}}{T_{v,j}}\right)\right] \tag{24}$$

for $j = H_3^+$

$$Z_{v,j} = \{1/[1 - \exp(-\theta_{v,ja}/T_{v,j})]\}\{1/[1 - \exp(-\theta_{v,jb}/T_{v,j})]\}^2 \tag{25}$$

$$\frac{\partial \ln Z_{v,j}}{\partial T_{v,j}} = \left(\frac{\theta_{v,ja}}{T_{v,j}^2}\right)\exp\left(\frac{-\theta_{v,ja}}{T_{v,j}}\right)\Big/\left[1 - \exp\left(\frac{-\theta_{v,ja}}{T_{v,j}}\right)\right] + 2\left(\frac{\theta_{v,jb}}{T_{v,j}^2}\right)\exp\left(\frac{-\theta_{v,jb}}{T_{v,j}}\right)\Big/\left[1 - \exp\left(\frac{-\theta_{v,jb}}{T_{v,j}}\right)\right] \tag{26}$$

where

$$\theta_{v,ja} = 1.43883 \times 3350 \text{ K} \tag{27}$$

$$\theta_{v,jb} = 1.43883 \times 2800 \text{ K} \tag{28}$$

The coefficients involved in the internal partition functions such as σ_j and $\theta_{\text{int},j}$ can be found in Huber and Herzberg's book[26] and the books edited by Glooshko.[27] The electronic excitation partition function and its derivative for hydrogen atom can be computed analytically. Z_{x,H_2} can be found in Patch's report.[10] A numerical derivative is employed to compute the derivative d Z_{x,H_2}/d T_{x,H_2} in the present calculation. Because of the extremely high energy levels of the excited states of H_2^+ and H_3^+,[28] only electronic ground states of these two species are considered in the electronic excitation mode.

The Debye-Huckel correction for multitemperature plasmas has been investigated in some detail. The change in free energy of a multitemperature plasma of density ρ and volume V is[12,29]:

$$\rho V A_{\text{corr}} = \frac{-e^2}{3\rho_D}\sum_j (N_j z_j^2) \tag{29}$$

Thus

$$a_{\text{corr},j} = -z_j^2 e^2/(3\rho_D) \tag{30}$$

where ρ_D is defined as

$$\rho_D = \left(\frac{4\pi e^2}{k}\sum_j \frac{z_j^2}{v_j T_{t,j}}\right)^{0.5} \tag{31}$$

The Debye-Huckel correction for the pressure of j is

$$p_{\text{corr},j} = \left.\frac{-\partial(\rho V A_{\text{corr},j})}{\partial V}\right|_{T_j,N_j} = \frac{-n_j z_j^2 e^2}{(6\rho_D)} \tag{32}$$

Therefore, the ideal gas law should be changed to

$$p_j v_j = kT_{t,j} + p_{\text{corr},j}/n_j = kT_{t,j} - z_j^2 e^2/(6\rho_D) \tag{33}$$

The Debye-Huckel correction for entropy is

$$s_{\text{corr},j} = \left.\frac{-\partial a_{\text{corr},j}}{\partial T_{t,j}}\right|_{v_j} \tag{34}$$

Since $a_{\text{corr},j}$ is a function of $v_1, v_2, \ldots, v_j, T_{t,1}, T_{t,2}, \ldots, T_{t,j}$, the derivative in Eq. (34) is carried out by keeping $v_1, v_2, \ldots, v_j, T_{t,1}, T_{t,2}, \ldots, T_{t,j-1}$ constant. The result is

$$s_{\text{corr},j} = \left(\frac{-z_j^2 e^2}{6\rho_D T_{t,j}}\right)\left(\frac{z_j^2}{v_j T_{t,j}}\right)\left(\sum_i \frac{z_i^2}{v_i T_{t,i}}\right)^{-1} \tag{35}$$

The Debye-Huckel correction terms are functions of the number densities and translational temperatures of electrons and heavy ions. Inclusion of the Debye-Huckel correction in the plasma model results in a small deviation from the ideal gas mixture model, which assumes the presence of different gases in a gas mixture has no effect on individual species. However in all the cases studied, the Debye-Huckel correc-

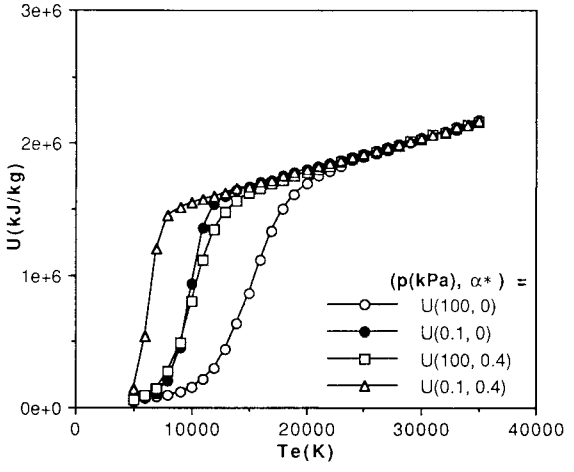

a) Internal energy

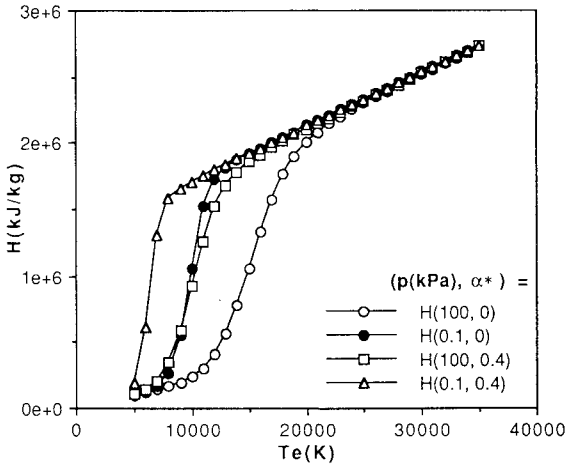

b) Enthalpy

Fig. 1 Internal energy and enthalpy vs T_e for LThE hydrogen plasmas at different pressures and dimensionless chemical affinities.

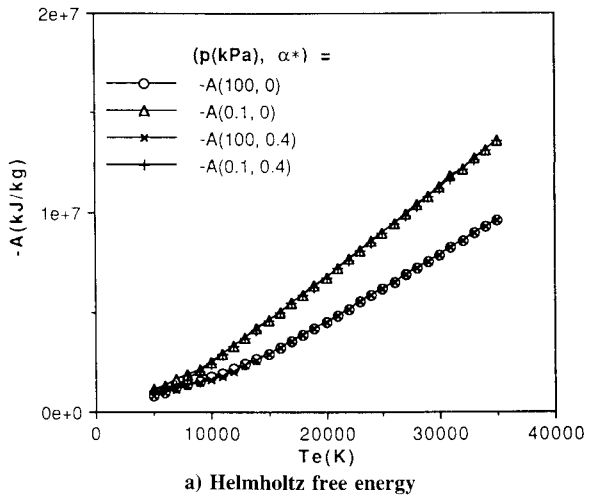

a) Helmholtz free energy

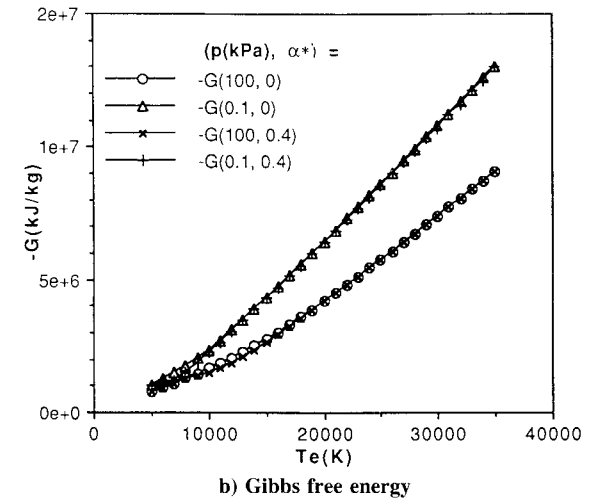

b) Gibbs free energy

Fig. 2 Helmholtz and Gibbs free energies vs T_e for LThE hydrogen plasmas at different pressures and dimensionless chemical affinities.

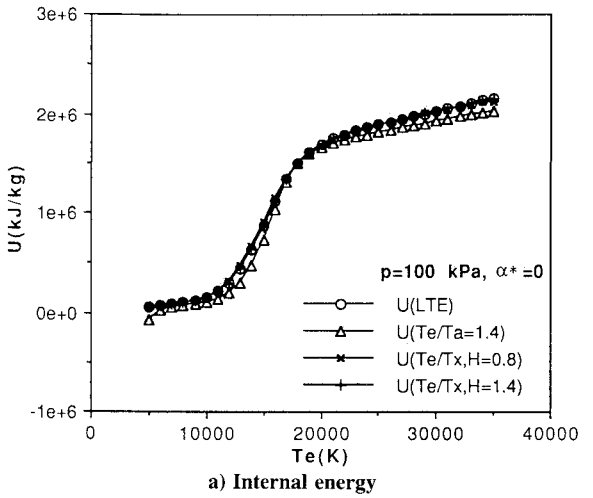

a) Internal energy

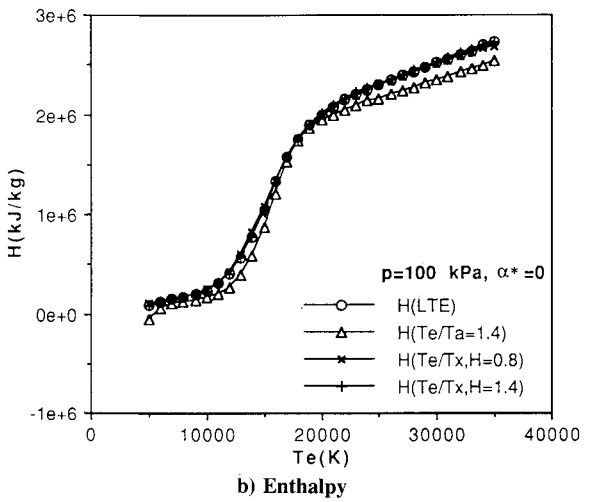

b) Enthalpy

Fig. 3 Effects of thermal nonequilibrium on internal energy and enthalpy.

tion was found to be very small. The difference between the computed thermodynamic properties and the results of an ideal gas mixture is therefore insignificant.

The speed of sound can be calculated from

$$c = \left(\frac{\partial p}{\partial \rho}\bigg|_s\right)^{0.5} \tag{36}$$

For an ideal gas

$$c = (\gamma RT)^{0.5} \tag{37}$$

where γ is the specific heat ratio. In a chemically reacting flow the specific heat consists of two terms, the frozen specific heat and the reactional specific heat.[30] The frozen term represents the sum of the contributions of each species and energy mode. The frozen specific heat of a particular energy mode can be calculated by differentiating the enthalpy or internal energy of that energy mode with respect to the associated temperature. The reactional specific heat is associated with chemical reactions. Since in a multitemperature plasma, chemical reactions depend on all the temperatures involved, it is difficult to find an appropriate temperature for the evaluation of the reactional specific heat. Consequently, we decided to use the numerical derivative of Eq. (36) with very small temperature and pressure increments to calculate the speed of sound of a nonequilibrium plasma.

Results and Discussion

The effects of changes in pressure and chemical affinity on enthalpy and internal energy are shown in Fig. 1 for a LThE hydrogen plasma (all temperatures are equal). The dominant chemical reaction in the temperature range considered is the recombination of hydrogen atoms. Compared to the LChE result ($\alpha^* = 0$), a positive α (or a positive α^* since H^0 of the recombination reaction is positive) results in higher H^+ and e^- concentrations than the LChE composition at a given temperature. Lowering the plasma pressure has similar effect. Since H^+ and e^- are at higher energy levels in comparison with H, enthalpy and internal energy increase drastically during ionization. After the plasma is fully ionized, H and U are independent of p and α^* and increase almost linearly with temperature, indicating the contribution of the translational mode dominates at high temperatures. On the other hand, the computed A and G (Fig. 2) show little effect of chemical nonequilibrium and decrease (note that the curves in Fig. 2 are negative A and G) at almost a constant rate as temperature increases for temperatures above 15,000 K. Change in pressure affects A and G significantly at high temperatures, as evidenced by the large difference between the curves of p = 0.1 and 100 kPa. But the difference becomes negligible as temperature drops to 5000 K.

The effects of thermal nonequilibrium on H, U, A, and G are shown in Figs. 3 and 4. Only temperature ratios not equal to unity are shown in the parentheses in the figures. Change in electronic excitation temperature seems to have no strong effect on these properties, as can be seen by comparing the result of $T_e/T_{x,H} = 0.8$ to that of $T_e/T_{x,H} = 1.4$. The effects of change in $T_{x,H}$ on H and U decrease after ionization of hydrogen atoms is completed. Increasing T_e while keeping T_a constant changes A, G, H, and U only slightly around 5000 K. But over the temperature range in which ionization takes

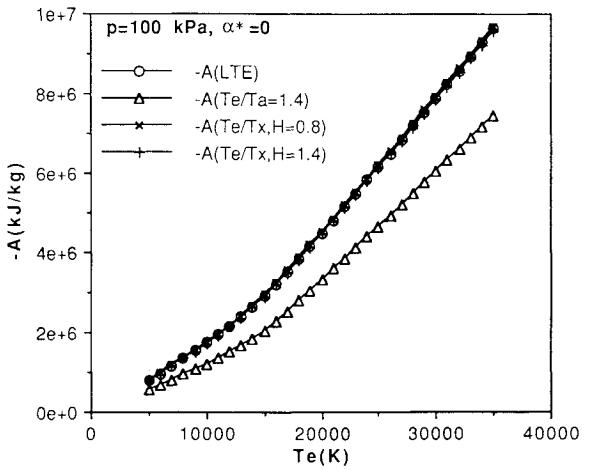

a) Helmholtz free energy

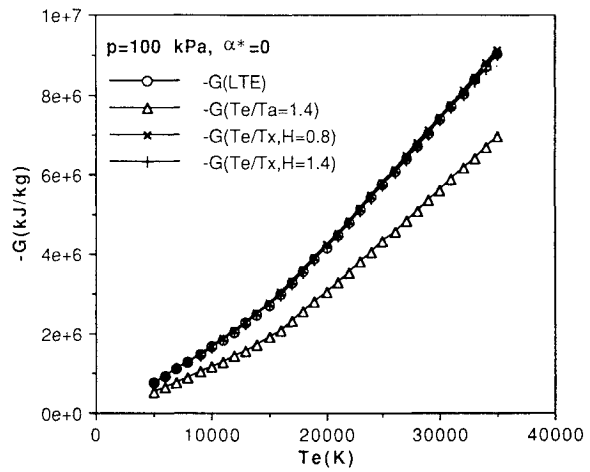

b) Gibbs free energy

Fig. 4 Effects of thermal nonequilibrium on Helmholtz and Gibbs free energies.

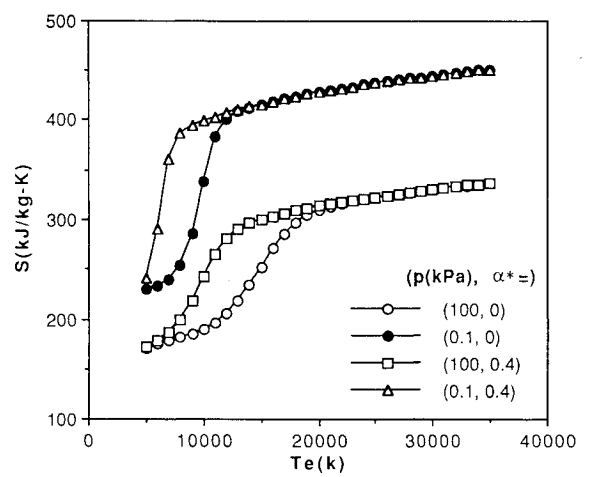

Fig. 5 Entropy vs T_e for LThE hydrogen plasmas at different pressures and dimensionless chemical affinities.

place, A, G, H, and U of $T_e/T_a = 1.4$ are much higher than those of $T_e/T_a = 1$ at a given T_a. Thus, increase in T_e has a great effect on plasma properties during ionization.

The effects of changes in p and α^* on entropy can be seen in Fig. 5. S increases as p decreases. Increase in α^* results in higher entropy during ionization. But different α^* values have no effect on S after ionization is completed. The effects of changes in temperatures of different energy modes on S for

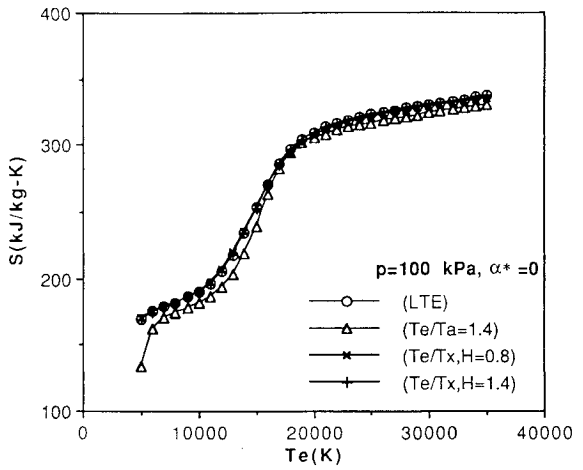

Fig. 6 Effects of thermal nonequilibrium on entropy.

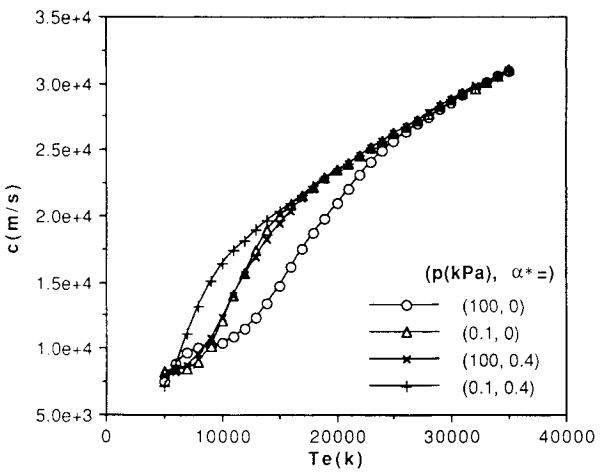

Fig. 7 Speed of sound vs T_e for LThE hydrogen plasmas at different p and α^*.

a LChE plasma ($\alpha^* = 0$) at 100 kPa are shown in Fig. 6. Change in $T_{x,H}$ has little effect on S. Change in T_e has a strong effect on S before ionization takes place. The entropy value for $T_e/T_a = 1.4$ is much less than those for $T_e/T_a = 1$ for temperatures below the ionization temperature. After hydrogen is fully ionized, the difference between different T_e/T_a ratios is small. In the temperature range in which ionization occurs, the computed entropy values for different T_e/T_a ratios show little difference at a given T_e. But S for $T_e/T_a = 1.4$ would be much higher than that for $T_e/T_a = 1$ if T_a were used to plot the entropy curves. Therefore, translational nonequilibrium is important to entropy calculation at temperatures above the ionization temperature.

The speed of sound of a nonequilibrium hydrogen plasma is calculated for a variety of pressure, temperature, and α^* combinations. The derivate of $\partial p/\partial \rho|_s$ is approximated by a three-point, central difference scheme along an isentropic line. Typical temperature and pressure increments used in the numerical derivate are 100 K and 1 (for $p = 100$ kPa) to 0.01 (for $p = 0.1$ kPa) kPa, respectively. Computed speed of sound for LTE hydrogen at 300–1000 K was compared to the ideal gas equation, Eq. (37), with γ computed from[31]

$$\gamma = c_p/(c_p - R) \tag{38}$$

$$c_p(kJ/kg \cdot K) = 56.505 - 702.74\theta^{-0.75} + 1165.0\theta^{-1} - 560.70\theta^{-1.5} \tag{39}$$

$$\theta = T(K)/100 \tag{40}$$

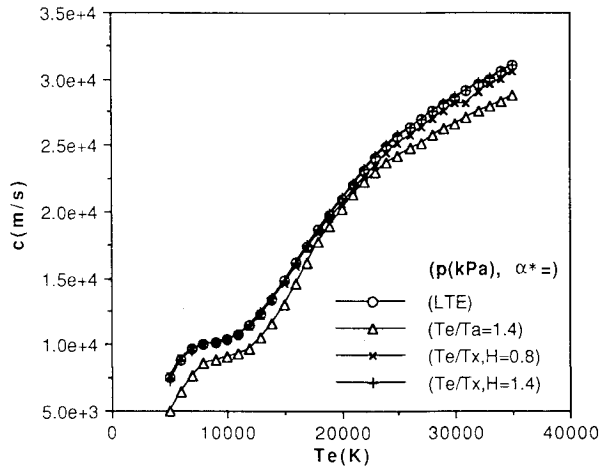

Fig. 8 Speed of sound vs T_e for LChE hydrogen plasmas in non-LThE.

The error was found to be less than 2%. Computed speed of sound for LTE hydrogen plasma in the full ionization region also agrees well with Cho's calculation[12] which was based on the method developed in Drellishak's paper.[32]

Shown in Fig. 7 are the speeds of sound for LThE hydrogen plasmas at $p = 0.1$ and 100 kPa, and $\alpha^* = 0$ and 0.4. Speed of sound increases with temperature and becomes independent of pressure after the plasma is fully ionized. The increase in speed of sound reaches a plateau when ionization takes place. Since ionization occurs at lower temperatures if p decreases or α^* increases, the plateaus in the sonic speed curves shift to lower T_e at low p or high α^*. Because the increase in c is frozen when chemical reactions take place, there exists a temperature range (T_e = 5000 to 10,000 K) in which the speed of sound decreases as p increases or α^* decreases. These plateaus were also found in the speed of sound calculation for argon plasma by Drellishak et al.[32]

Shown in Fig. 8 are the speeds of sound for different temperature ratios. It is shown in this figure that change in electronic excitation temperature has no effect on c until very high temperatures are reached. Changes in translational temperature ratios, on the other hand, have a strong effect on the speed of sound, especially in the temperature range in which ionization takes place.

Conclusion

A nonequilibrium plasma model has been developed and a computer program written for computing the thermodynamic properties and speed of sound of molecular hydrogen in both non-LThE and non-LChE. This type of computer program is useful as a subroutine to a computational fluid dynamics code, for comparing species density and property variations from LTE, and for determining simplifications in diagnostics and modeling. It is found that a decrease in plasma pressure or a positive affinity of the recombination of hydrogen atoms causes ionization to occur at lower temperatures, resulting in higher plasma enthalpy, internal energy, and entropy. But chemical nonequilibrium has little effect on A and G. On the other hand, pressure change has a strong effect on A and G. H and U are independent of p and α^* after ionization is completed. Of the different energy modes, the translational mode plays a dominant role for hydrogen from 5000 to 35,000 K. Change in T_e affects U, H, and S significantly during ionization. The speed of sound increases primarily with the translational temperatures. Frozen speed of sound is found when chemical reactions take place.

Acknowledgments

K. Chen would like to thank the Associated Western Universities, Inc. and the Department of Energy (Contract DE-AC07-76ID01570) for the sponsor of two Summer Faculty Fellowships at the Idaho National Engineering Laboratory.

References

[1]Pierce, F. J., *Microscopic Thermodynamics*, International Textbook, Scranton, PA, 1968, pp. 364–367.

[2]Anderson, J. D., *Modern Compressible Flow with Historical Perspective*, 1st ed., McGraw-Hill, New York, 1982, pp. 334–433.

[3]Eddy, T. L., Grandy, J. D., and Detering, B. A., "Chemical Nonequilibrium in an Argon Plasma Torch Plume," *Heat Transfer in Thermal Plasma Processing*, American Society of Mechanical Engineers, HTD-Vol. 161, New York, 1991, pp. 79–88.

[4]Haase, R., *Thermodynamics of Irreversible Processes*, Addison-Wesley, Reading, MA, 1969 and Dover, New York, 1990, pp. 39–156.

[5]Rosenbaum, B. M., and Levitt, L., "Thermodynamic Properties of Hydrogen from Room Temperature to 100,000 °K," NASA TN D-1107, Jan. 1962.

[6]Krascella, N. L., "Tables of the Composition, Opacity, and Thermodynamic Properties of Hydrogen at High Temperatures," NASA SP-3005, Sept. 1963.

[7]Harris, G. M., "Equilibrium Properties and Equation of State of a Hydrogen Plasma," *Physical Review*, Vol. 133, No. 2A, 1964, pp. 427–435.

[8]Fisher, B. B., "Calculation of the Thermal Properties of Hydrogen," Los Alamos Scientific Lab., Rept. LA-3364, Los Alamos, NM, 1966.

[9]Patch, R. W., and McBride, B. J., "Partition Functions and Thermodynamic Properties to High Temperatures for H_3^+ and H_2^+," NASA TN D-4523, April 1968.

[10]Patch, R. W., "Components of a Hydrogen Plasma Including Minor Species," NASA TN D-4993, Jan. 1969.

[11]King, C. R., "Compilation of Thermodynamic Properties, Transport Properties, and Theoretical Rocket Performance of Gaseous Hydrogen," NASA TN D-275, April 1960.

[12]Cho, K. Y., "Nonequilibrium Thermodynamic Models and Applications to Hydrogen Plasma," Ph.D. Dissertation, Dept. of Mechanical Engineering, Georgia Inst. of Tech., Atlanta, GA, 1988.

[13]Patch, R. W., "Thermodynamic Properties and Theoretical Rocket Performance of Hydrogen to 100000 K and 1.01325 × 10^8 N/m^2," NASA SP-3069, June 1971.

[14]Chen, K., and Eddy, T. L., "Composition and Partition Functions of a Hydrogen Plasma in Thermal and Chemical Nonequilibrium," DOE Rept. EGG-SCM-10420, 1992.

[15]Chen, K., and Eddy, T. L., "Composition and Partition Functions of Partially Ionized Hydrogen Plasma in Non-Local Thermal Equilibrium (Non-LThE) and Non-Local Chemical Equilibrium (Non-LChE)," *Heat Transfer in Thermal Plasma Processing*, American Society of Mechancial Engineers, HTD-Vol. 161, New York, 1991, pp. 177–185.

[16]De Donder, Th., *L'Affinité*, 1^{ve} 'ed, Paris, Gauthier-Villars, 1927.

[17]Prigogine, I., "Extension de l'Equation de Saha au Plasma Non-Isotherme," *Bulletin de la Classe des Sciences, Academie Royale de Belgique.*, Vol. 26, 1940, pp. 53–63.

[18]Potapov, A. V., "Chemical Equilibrium of Multitemperature Systems," *High Temperature*, Vol. 4, 1966, pp. 48–51.

[19]Samuilova, E. V., "Trapping Cross Sections of Electrons with Respect to Spherical Particles and Thermal Ionization of the Particles," *High Temperature*, Vol. 4, 1966, pp. 139–143.

[20]Veis, S., "The Saha Equation and the Lowering of the Ionization Energy for a Two-Temperature Plasma," *Czechoslovak Conference on Electronic and Vacuum Physics*, Paper A3-1, Prague, 1968, pp. 105–110.

[21]Bott, J. F., "Spectroscopic Measurement of Temperature in an Argon Plasma Arc," *Physics of Fluids*, Vol. 9, No. 8, 1966, pp. 1540–1547.

[22]Callen, H. B., *Thermodynamics and an Introduction to Thermostatistics*, 2nd ed., Wiley, New York, 1985, pp. 307–314.

[23]De Donder, Th., and Van Rysselberghe, P., *Thermodynamic Theory of Affinity*, Stanford Univ. Press, Stanford, CA, 1936, pp. 2–41.

[24]Eddy, T. L., and Cho, K. Y., "A Multitemperature Model for Plasmas in Chemical Nonequilibrium," *Heat Transfer in Thermal Plasma Processing*, American Society of Mechanical Engineers, HTD-Vol. 161, New York, 1991, pp. 195–210.

[25]Eddy, T. L, Detering, B. A., and Wilson, G. C., "LTE and Non-

LTE Gas Temperatures in Loaded and Unloaded Plasmas During Spraying of NiAl Powders," *Thermal Spray Research and Applications*, American Society for Metals International, Materials Park, OH, 1991, pp. 33–37.

[26]Huber, K. D., and Herzberg, G., *Molecular Spectra and Molecular Structure, Part IV: Constants of Diatomic Molecules*, Van Nostrand Reinhold, Princeton, NJ, 1979, pp. 240–275.

[27]Glooshko, V. P. (ed.), *Thermodynamic Properties of Individual Substances* (in Russian), Science Publishing House in Moscow, Moscow, Vol. 1, No. 1, 1978, p. 110.

[28]Sharp, T., *Atomic Data*, Vol. 2, Academic Press, New York, 1971, p. 119.

[29]Davidson, N. R., *Statistical Mechanics*, McGraw-Hill, New York, 1962, p. 485.

[30]Fauchais, P., "Fundamental Concepts," *Thermal Plasmas*, edited by S. Veprek, International Summer School on Plasma Chemistry, Atami, Japan, 1987, pp. 1–64.

[31]Van Wylen, G., and Sonntag, R. E., *Fundamentals of Classical Thermodynamics*, 3rd ed., Wiley, New York, 1986, p. 688.

[32]Drellishak, K. S., Knop, C. F., and Cambel, A. B., "Partition Functions and Thermodynamic Properties of Argon Plasma," *Physics of Fluids*, Vol. 6, No. 9, 1963, pp. 1280–1288.